Applied Microbiology and Biotechnology (2024) 108:305
https://doi.org/10.1007/s00253-024-13144-z

BIOTECHNOLOGICALLY RELEVANT ENZYMES AND PROTEINS

Application of an alchemical free energy method for the prediction of thermostable DuraPETase variants

Sebastian Schreiber[1] · David Gercke[1] · Florian Lenz[1] · Joachim Jose[1]

Received: 16 January 2024 / Revised: 25 March 2024 / Accepted: 9 April 2024 / Published online: 21 April 2024

Abstract

Non-equilibrium (NEQ) alchemical free energy calculations are an emerging tool for accurately predicting changes in protein folding free energy resulting from amino acid mutations. In this study, this method in combination with the Rosetta *ddg monomer* tool was applied to predict more thermostable variants of the polyethylene terephthalate (PET) degrading enzyme DuraPETase. The Rosetta *ddg monomer* tool efficiently enriched promising mutations prior to more accurate prediction by NEQ alchemical free energy calculations. The relative change in folding free energy of 96 single amino acid mutations was calculated by NEQ alchemical free energy calculation. Experimental validation of ten of the highest scoring variants identified two mutations (DuraPETase^{S61M} and DuraPETase^{S223Y}) that increased the melting temperature (T_m) of the enzyme by up to 1 °C. The calculated relative change in folding free energy showed an excellent correlation with experimentally determined T_m resulting in a Pearson's correlation coefficient of $r = -0.84$. Limitations in the prediction of strongly stabilizing mutations were, however, encountered and are discussed. Despite these challenges, this study demonstrates the practical applicability of NEQ alchemical free energy calculations in prospective enzyme engineering projects.

Key points

- *Rosetta ddg monomer enriches stabilizing mutations in a library of DuraPETase variants*
- *NEQ free energy calculations accurately predict changes in T_m of DuraPETase*
- *The DuraPETase variants S223Y, S42M, and S61M have increased T_m*

Keywords Alchemical free energy calculations · Enzyme engineering · Thermostability · MD simulation · PETase

Introduction

Enhancing the thermostability of enzymes is a key aspect in the field of enzyme engineering as biotechnological and industrial application processes require highly stable enzymes (Bommarius et al. 2011; Nezhad et al. 2022). Directed evolution has proven to be a successful approach for developing thermostable proteins (Labrou 2010). It is, however, labor intensive and screening of a large number of enzyme variants is necessary. This makes this approach expensive and limits it to enzymes for which high-throughput assays are available. Computational methods that can aid in protein or enzyme design to reduce the screening efforts have therefore gained popularity. Software tools such as FoldX, RosettaDesign, or PoPMuSiC 2.1 make use of semi-empirical force fields to predict the change in folding free energy ($\Delta\Delta G_{folding}$) of given mutations (Dehouck et al. 2009; Guerois et al. 2002; Kellogg et al. 2011). $\Delta\Delta G_{folding}$ gives the difference in $\Delta G_{folding}$ between a wild-type and a mutant protein, whereas $\Delta G_{folding}$ is the difference in free energy between the unfolded and the folded states. The prediction accuracy of these methods is however highly dependent on the investigated protein (Buß et al. 2018). Most of the time, a relatively high number of predictions still need to be tested to identify more stable variants (Wijma et al. 2014). Nevertheless, semi-empirical force field-based methods usually perform better than random selection of mutations (Buß et al. 2018). These predictions are often complemented by molecular dynamic (MD) simulations with subsequent analysis of the protein's flexibility and/or hydrophobic

Sebastian Schreiber and David Gercke contributed equally.

✉ Joachim Jose
joachim.jose@uni-muenster.de

[1] University of Münster, Institute of Pharmaceutical and Medicinal Chemistry, PharmaCampus, Corrensstr. 48, 48149 Münster, Germany

surface area (Childers and Daggett 2017; Floor et al. 2014; Wang et al. 2018). The results attained from MD simulations are however difficult to analyze objectively, since analysis is dependent on correct visual inspection and interpretation of the MD trajectory (Wijma et al. 2014). In recent years, physically rigorous free energy calculations emerged as a promising new tool for the prediction of $\Delta\Delta G_{\text{folding}}$. When using this method to calculate $\Delta\Delta G_{\text{folding}}$ in a conventional, non-alchemical way, sampling of the complete folding or unfolding path of each variant is necessary. Even though this is possible in principle, it requires a lot of computational effort and is therefore often not feasible. Alchemical free energy calculations are physically rigorous calculations that circumvent this problem by estimating free energy differences along nonphysical, so-called alchemical paths that are more accessible to sampling by MD or Monte Carlo simulations. This way, alchemical free energy methods account for solvent effects, conformational changes, and electrostatic interactions with higher precision than semi-empirical methods. Several different approaches to alchemical free energy calculations have been developed and used in the past. Among the most popular is the free energy perturbation method based on the principles first published by Zwanzig (1954). Using this method, equilibrium simulations for several intermediate states along the alchemical path are simulated. From these, free energy differences are then estimated (Bennett 1976; Shirts and Chodera 2008). This approach has been implemented in the Schrödinger molecular modeling suite and has been used in several publications to accurately predict $\Delta\Delta G_{\text{folding}}$ or protein–protein interaction free energies upon amino acid mutation (Ford and Babaoglu 2017; Steinbrecher et al. 2017a, 2017b). It is, however, also possible to derive free energy differences from non-equilibrium simulations (NEQ) (Crooks 1999; Jarzynski 1997a, b). This was made easily accessibly within the GROMACS framework over the last couple of years by the group around de Groot (Gapsys et al. 2015b; Seeliger and de Groot 2010). This approach has been shown to give good prediction accuracy in retrospective studies, in which literature values were used to verify the validity of the predictions. Recently, the approach was also used prospectively to guide the functional analysis of a disease conferring mutation in the proliferating cell nuclear antigen followed by experimental validation (Hardebeck et al. 2023). Prospective, larger scale studies employing this method for the prediction of more thermostable enzyme variants, followed by experimental validation, are however scarce. We therefore decided to test the ability of a workflow based on NEQ alchemical free energy calculations to improve the thermal stability of a biotechnologically relevant enzyme. The development of solutions for the environmental burden of polyethylene terephthalate (PET) remains a daunting challenge (Yoshida et al. 2016). For the degradation of PET, the use of highly active biocatalysts is a promising approach. Since PET degradation is most efficient near the glass transition temperature of PET (ca. 70 °C), increasing the thermostability of the PET-degrading enzyme *Is*PETase is crucial for the efficient application of the enzyme in industrial processes (Jog 1995; Wei and Zimmermann 2017). Significant efforts have already been made to optimize and improve *Is*PETase (Bell et al. 2022; Brott et al. 2022; Liu et al. 2022; Lu et al. 2022; Shi et al. 2023; Zurier and Goddard 2023). DuraPETase is one of the most thermostable variants, with one of the highest PET degradation rates known today (Cui et al. 2021). It was created by experimentally testing and combining a library of 85 different mutations. This resulted in a thermostable enzyme variant of mesophilic PETase with ten additional point mutations and a T_m elevated by 31 to 78 °C. Further improvement of DuraPETase should therefore pose an interesting and challenging test case for the performance of the NEQ alchemical free energy approach.

Here, we present a study that utilizes NEQ alchemical free energy calculations prospectively to identify variants of DuraPETase with enhanced thermostability. We systematically evaluated the performance of two computational methods, Rosetta *ddg monomer* and NEQ free energy calculations, for the prediction of more thermostable variants of the highly thermostable DuraPETase. Calculations with Rosetta *ddg monomer* proved to be able to enrich stabilizing mutations. However, predictions did not significantly correlate with experimentally determined T_m. $\Delta\Delta G_{\text{folding}}$ of 23 DuraPETase variants (Table S1) predicted by NEQ free energy calculations correlated well with experimentally determined T_m with a Pearson's correlation coefficient of $r = -0.84$. Among these variants, two variants (DuraPETase^{S61M} and DuraPETase^{S223Y}) had increased T_m by up to 1 °C compared to the original DuraPETase.

Material and methods

Plasmid construction, mutagenesis, expression, and protein purification

The sequence of DuraPETase (GenBank: GAP38373.1) was codon optimized for *E.* coli and synthesized by Twist Bioscience (South San Francisco, USA). The codon-optimized sequence of the DuraPETase gene is given in Sequence S1. It was inserted into the plasmid p15-mNeonGreen (Hardebeck et al. 2023) by restriction and ligation to create the plasmid pDuraPETase for intracellular expression of the original DuraPETase under control of a T7 promotor. Point mutations for the generation of DuraPETase variants were introduced by PCR via In-Fusion cloning (Takara Bio, Kusatsu, Japan). *E. coli* BL21(DE3) was used as the host for protein expression. Cells containing one of the respective plasmids for the expression of the original DuraPETase or its

variants were grown in 500 ml lysogeny broth-Miller (LB) medium supplemented with 50 µg/ml carbenicillin at 33 °C and 160 rpm. Gene expression was induced with 1 mM IPTG as soon as an optical density at 578 nm of 0.8 was reached and incubation was continued for 24 h at 16 °C and 160 rpm. Cells were harvested by centrifugation (5000 × g, 10 min, 4 °C), suspended in 5 ml loading buffer (50 mM NaH_2PO_4, 300 mM NaCl, 10 mM imidazole, pH 8), and lysed using a sonicator. Cell debris were removed by centrifugation (48,000 × g, 15 min, 4 °C). The supernatant was used to isolate the respective enzyme via Ni–NTA affinity chromatography using Protino Ni–NTA agarose beads (Th. Geyer, Höxter, Germany), and the buffer was exchanged for storage buffer (50 mM Na_2HPO_4-Hcl, pH 7, 100 mM NaCl) by dialysis. Enzyme concentrations were determined by measuring the absorbance at 280 nm.

Differential scanning fluorimetry (DSF)

To determine the apparent T_m of the original DuraPETase and its variants by DSF, 4 µM of the respective enzyme in 25 µl of PBS containing a total of 20 × SYPRO orange protein gel stain (Sigma-Aldrich, St. Louis, USA) and a Rotor-Gene Q 2 Plex HRM (Qiagen, Hilden, Germany) were used (Lavinder et al. 2009). The samples were heated from 30 to 95 °C, increasing the temperature by 0.5 °C every 5 s. SYPRO orange was excited at 470 ± 10 nm, and the emission was detected at 610 ± 5 nm. All measurements were performed three times from individually prepared samples. The apparent T_m were calculated from the extreme points of the first derivative of the fluorescence dF/DT(T) formed from the recorded melting curves as function F(T) using the Rotor-Gene Q software.

Determination of PET degradation rates

The PET degradation rates for the original DuraPETase and its variants were tested using amorphous PET (2.4% crystallinity, determined by differential scanning calorimetry) with a thickness of 0.25 mm purchased from Goodfellow Cambridge Limited (Huntingdon, England). Substrate cut-outs with a diameter of 6 mm were incubated in 300 µl of 50 mM bicine NaOH buffer pH 9 containing 100 nM of the respective enzyme in microvolume reaction tubes. All reactions were performed as triplicates and were incubated at 50 °C or 52 °C and 300 rpm for 3 days. The reactions were stopped by removing the substrate. Three volumes of acetonitrile were added, and a centrifugation step (20,000 × g, 10 min) was performed. For each sample, 10 µl of the supernatant was injected into a LaChrom Elite HPLC system equipped with a L-2455 DAD detector (Hitachi, Chiyoda, Japan) and a Nucleodur C18 HTec column (Macherey–Nagel, Düren, Germany). The separation was performed isocratically at 40 °C with a flow rate of 0.5 ml/min for 8 min using 70% ddH_2O, 20% acetonitrile, and 10% formic acid. The signal was detected at 254 nm, and standards of the reaction products terephthalic acid (TCI, Tokyo, Japan) and 2-hydroxyethyl terephthalic acid (Activate Scientific, Prien am Chiemsee, Germany) were used to quantify the degradation rate.

Rosetta ddg monomer calculations

Rosetta version 3.12 was used for the *ddg monomer* calculations. The crystal structure of DuraPETase (PDB ID: 6ky5) was used for all calculations. Only chain A was retained. Ions and water molecules were deleted. First, minimization was performed using distance constrains on Cα atoms. The protocol described as "row 3" in Kellogg et al. was used for all calculations. This protocol was chosen, because it exhibited a high prediction accuracy for the dataset analyzed in the original publication (Kellog et al. 2011), while also appeared to be computationally inexpensive. The commands are described in detail in the Supporting information of Kellogg et al. (2011).

NEQ alchemical free energy calculations

System preparation

The crystal structure of DuraPETase (PDB ID: 6ky5) was retrieved from the PDB server. Only chain A was retained. Ions and water molecules were deleted. Protonation states were assigned with the Protonate 3D function from MOE (Molecular Operating Environment, Chemical Computing Group, Canada version: 2022.02) using default settings at pH = 7.0. Mutations were generated using the Protein Builder. Sidechains were repacked and minimized using the Minimize tool, while a tether was applied to the backbone. The structures were exported from MOE in PDB format and used for MD system preparation within GROMACS 2019.3 (Abraham et al. 2015).

Free energy calculations and hybrid topology generation

For the estimation of the change in folding free energy ($\Delta\Delta G_{folding}$) upon amino acid mutation, a well-established thermodynamic cycle was constructed according to Aldeghi et al. (2019). The cycle is also shown in Figure S1 for clarity. The alchemical transitions between both end states were performed along the ΔG_1 arrow for the unfolded and along the ΔG_3 arrow for the folded state. The unfolded state was modeled by a Gly-X-Gly tripeptide as done in previous publications (Gapsys et al. 2015b, 2016). All simulations were run independently from each other. The pmx

package was used to generate hybrid topologies (Gapsys et al. 2015b). This was done after equilibrium simulations were performed. This way, equilibrium trajectories of the original DuraPETase could be used for different amino acid transitions.

Molecular dynamic (MD) simulations

GROMACS 2019.3 was used to carry out all MD simulations (Abraham et al. 2015). The Amber99SB*ILDN force field was used to model the protein (Lindorff-Larsen et al. 2010). Water molecules were represented by the TIP3P water model. Proteins or tripeptides were solvated in a cubic box with 150 mM of Na^+ and Cl^- ions. The total charge of the system was neutralized with either Na^+ or Cl^-. For equilibrium simulations, energy minimization was performed using the steepest decent method. Equilibration was performed for 500 ps in the NVT and for 500 ps in the NPT ensemble. A position restraint with a value for the harmonic force constants of 1000 kJ mol^{-1} nm^{-2} was applied to all heavy atoms of the system during both equilibration phases. Production simulations were run for 10 ns. H-Bonds were constrained using LINCS algorithm (Hess et al. 1997), and the simulation temperature was controlled by the velocity rescaling thermostat at 300 K every 0.1 ps (Bussi et al. 2007). The Parrinello-Rahman barostat was used to control pressure at 1 atm (Parrinello and Rahman 1981). Particle mesh Ewald was used to treat electrostatic interactions in the simulation with a cutoff set to 1.2 nm (Essmann et al. 1995). The mean RMSD during the production stage of each replica was calculated to check the system stability.

After equilibrium simulation, snapshots were extracted to construct hybrid topologies and perform the NEQ transition simulations. To do so, the first 2.5 ns of each trajectory was discarded and 75 snapshots were extracted equidistantly from the remaining trajectory. The pmx package was used to generate hybrid topologies (Gapsys et al. 2015b). Transitions were performed in 100 ps after energy minimization and 50 ps of equilibration. The resulting change in λ was 5×10^{-5}/step. A softcore potential with default parameters was applied to the Lennard–Jones and electrostatic interactions. Using the scripts provided with the pmx package, extracted work values were used to estimate the free energy at 300 K. The free energy estimation was based on the Crooks fluctuation theorem (Crooks 1999). Bennett acceptance ratio was used as a maximum likelihood estimator (Shirts et al. 2003). The uncertainty given is the standard deviation over multiple independent replicas. Either ten or four independent replicas were used at different stages of the study as stated in the "Results" section.

Results

In silico screening for stabilizing mutations in DuraPETase using ddg monomer

The high computational demand of alchemical free energy calculations is one of its drawbacks and makes comprehensive screening of the entire mutational space of a protein practically impossible in the foreseeable future. Semi-empirical force field-based methods provide a fast alternative to systematically analyze single-point mutations of the entire protein. We therefore decided to include a first virtual screening step using the Rosetta *ddg monomer* tool in the optimization of thermostability of DuraPETase (Kellogg et al. 2011). This also provided the opportunity to test, whether further improvement of the thermostability of DuraPETase could be achieved using this simpler approach. A systematic screening of all possible single amino acid mutations, with some exceptions, was performed. Firstly, mutations from and to proline are not supported by the later employed NEQ free energy calculations at the moment. They were therefore excluded in this step. Secondly, mutations involving the catalytic triad of DuraPETase were also excluded, as these amino acids are essential for catalytic activity. Lastly, charge change mutations were shown to be poorly predicted by the ddg monomer approach (Gapsys et al. 2016). Charge change mutations also need to be setup in a slightly different way for the NEQ free energy calculations due to artifacts introduced by a net charge change. Additionally, even if properly set up, charge change mutations still require substantially longer to reach convergence during the simulation (Patel et al. 2021). Taking all of this into account, we decided to exclude charge change mutations from our screening. In the end, this resulted in a total of 2838 single amino acid mutations for the 264 amino acids comprising DuraPETase. The change in folding free energy of these mutations was calculated with *ddg monomer* employing the row 3 protocol from Kellogg et al. (2011). These calculations were completed in a single day on a medium-sized cluster. Mutations were then ranked according to their score, which is intended to correlate with $\Delta\Delta G$ but is not a quantitatively predicted change in folding free energy (Fig. 1a). The score calculated with *ddg monomer* will be named $\Delta\Delta G_{\text{Rosetta}}$ in the following to distinguish it from the $\Delta\Delta G_{\text{folding}}$ determined by NEQ alchemical free energy calculations. Cutoff values varying from < -0.75 to < -5 kcal/mol are often used to identify stabilizing mutations (Buß et al. 2018; Wijma et al. 2014). The cutoff for the mutational scan of DuraPETase was set to $\Delta\Delta G_{\text{Rosetta}} < -3.8$ kcal/mol. This was within the normally

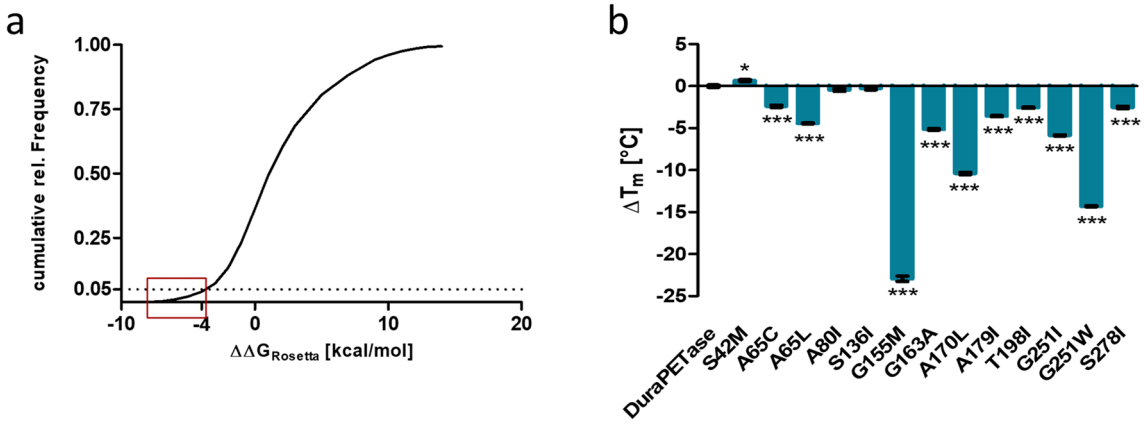

Fig. 1 **a** Cumulative distribution of *ddg monomer* results predicting the change in folding free energy upon amino acid mutation of DuraPETase. Mutations from and to proline, mutations involving a net charge change, and mutations involving the catalytic triad were excluded. The red box indicates the 130 variants below the cutoff value of $\Delta\Delta G_{Rosetta} < -3.8$ kcal/mol from which 13 were randomly selected for experimental validation. **b** ΔT_m were calculated by subtracting the T_m value of the original DuraPETase from the T_m value of each respective variant. T_m values were determined by DSF. The variants were randomly selected among the variants within the top 5% of predictions made with *ddg monomer*. Measurements were performed in triplicate. Statistical significance was analyzed by one-way ANOVA with Dunnett's multiple comparison test. Single asterisk (*) corresponds to $p < 0.05$ and triple asterisk (***) corresponds to $p < 0.001$

chosen range of cutoff values and comprises the top 5% of the scores corresponding to 130 different DuraPETase variants. These variants should next be characterized experimentally. As our laboratory capacities did not allow for the purification and characterization of around 130 different DuraPETase variants, 13 variants were chosen randomly from below the threshold for experimental verification. Variants were purified by Ni–NTA affinity chromatography. The respective change in the apparent melting temperatures (ΔT_m) for each variant compared to the original DuraPETase was calculated by substracting the T_m of the original DuraPETase from the T_m of the variant. Both T_m were measured by differential scanning fluorimetry (DSF) (Fig. 1b). Only a single variant, DuraPETase^{S42M}, had a significantly higher T_m than the original DuraPETase. The T_m of the DuraPETase^{S42M} variant was 0.66 ± 0.17 °C higher. The T_m of DuraPETase^{S136I} and DuraPETase^{A80I} did not differ from the original DuraPETase. All other variants had significantly lower T_m when compared to the original DuraPETase. Consequently, the success rate was low. The prediction accuracy was also rather poor, as four of the mutations (DuraPETase^{G155M}, DuraPETase^{A170L}, DuraPETase^{G251I}, and DuraPETase^{G251W}) predicted to be stabilizing were destabilized by more than 5 °C. Due to the low prediction accuracy, a set of 13 DuraPETase variants with a wide range of T_m was obtained, providing a reasonable dataset that was used to test the accuracy of NEQ free energy calculations for the DuraPETase in a next step.

Prediction accuracy of NEQ free energy calculations of DuraPETase

In order to analyze how well the results from the experimental testing could be calculated with NEQ free energy calculations, these calculations were performed for all of the 13 variants that were tested experimentally in the first screening round (Fig. 1b). Ten independent calculations were performed for each amino acid mutation using equilibrium trajectories of 10 ns in order to obtain a reliable estimate of uncertainty. Previous research has shown that running several short simulations results in more accurate error estimates than running fewer long simulations (Bhati and Coveney 2022). Analysis of the mean RMSD of the original DuraPETase confirmed the stability of the system during equilibrium MD simulation (Supplementary Figure S2). The hybrid topologies for the NEQ transitions were constructed after running the equilibrium trajectories, as explained in the "Material and methods" section. This way, the equilibrium trajectories of the original DuraPETase could be used for all transitions, which substantially reduced computational cost. NEQ free energy calculations are easily scalable, as the many short non-equilibrium transitions can be run independently. This way, calculations could be performed relatively quickly in approx. 3 days, on a medium-sized cluster. Predicted $\Delta\Delta G_{folding}$ was obtained as the result of the calculation. Figure 2 shows the correlation between the predicted $\Delta\Delta G_{folding}$ and the experimentally determined ΔT_m of the 13 DuraPETase variants described above. A significant Pearson

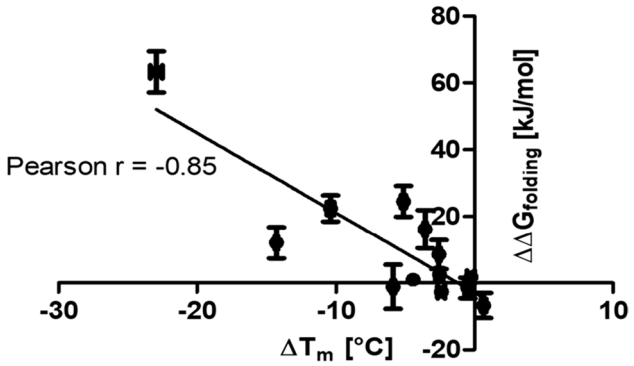

Fig. 2 Experimentally determined ΔT_m plotted against $\Delta\Delta G_{folding}$ calculated by NEQ free energy calculations of 13 DuraPETase variants. ΔT_m were calculated by subtracting the T_m value of the original DuraPETase from the T_m value of each respective variant. T_m values were determined by DSF. The uncertainty given is the standard deviation of three independent measurements. The uncertainty of $\Delta\Delta G_{folding}$ for each mutation is the standard deviation of ten independent replicas. A significant negative correlation between ΔT_m and $\Delta\Delta G_{folding}$ was observed (Pearson r = -0.85, p = 0.002, N = 13). Linear regression (black line) gave an R^2 = 0.70

correlation between $\Delta\Delta G_{folding}$ and ΔT_m of $r = -0.84$ was determined. Linear regression gave an $R^2 = 0.70$. A negative correlation was expected, as higher or more positive $\Delta\Delta G_{folding}$ values correspond to thermodynamically unstable proteins. These proteins have a lower T_m and therefore a negative ΔT_m. Even though ten replicas were used for $\Delta\Delta G_{folding}$ calculations, the prediction accuracy for the 13 DuraPETase mutations also remained consistent when using only four randomly selected replicas. Therefore, it should be sufficient in this case to run only four replicas per prediction for further calculations to reduce the computational burden. It is worth noting that our dataset is biased towards predominantly destabilizing mutations. It is therefore especially encouraging that DuraPETase^{S42M}, which is the only stabilizing mutation, is predicted with $\Delta\Delta G_{folding} = -6.7$ kJ/mol, the lowest among the predictions. Overall, we concluded that NEQ free energy calculations can identify stabilizing mutations in DuraPETase.

Two-step screening approach using ddg monomer and NEQ free energy calculations

Free energy changes calculated by NEQ free energy calculations showed a strong correlation with experimentally determined T_m but are computationally demanding. We therefore aimed to determine if the results of the *ddg monomer* calculations could serve as an initial screening tool to enrich promising mutations for further investigation. Twenty single amino acid mutations were selected from the *ddg monomer* prediction pool of 801 predictions having a $\Delta\Delta G_{Rosetta}$ exceeding 4 kcal/mol. Another 20 were selected from a pool of 2037 predictions with a $\Delta\Delta G_{Rosetta}$ lower than 4 kcal/mol. This cutoff was selected to test whether Rosetta *ddg monomer* could differentiate destabilizing mutations from stabilizing or neutral ones. The subsets were labelled "high" and "low," respectively. NEQ free energy calculations were used to predict $\Delta\Delta G_{folding}$ for each individual amino acid mutation in both groups. The simulations for one mutation in the *high* subset did not converge properly, as evident by the insufficient overlap in the work distribution to estimate ΔG. This mutation was excluded from further analysis. Thus, the resulting dataset consisted of 39 data points. The mean $\Delta\Delta G_{folding}$ calculated with the NEQ alchemical free energy workflow was compared between the *high* and *low* datasets (Fig. 3a). The mean $\Delta\Delta G_{folding}$ for all predictions derived from the *high* subset was 21.18 ± 5.36 kJ/mol. In contrast, the mean $\Delta\Delta G_{folding}$ for all predictions from the *low* subset was 4.01 ± 4.53 kJ/mol. This difference was statistically significant ($p = 0.020$). The four most negative $\Delta\Delta G_{folding}$ predictions all belonged to the *low* subset. Subsequently, $\Delta\Delta G_{folding}$ values, which were calculated with the NEQ free energy protocol, were plotted against $\Delta\Delta G_{Rosetta}$ for every single amino acid mutation (Fig. 3b). The $\Delta\Delta G_{Rosetta}$ and $\Delta\Delta G_{folding}$ were significantly correlated with Pearson's correlation coefficient of $r = 0.39$. Consequently, $\Delta\Delta G_{Rosetta}$ can provide a rough estimation of the impact of a single amino acid mutation on protein stability. This suggests that *ddg monomer* can serve as an initial enrichment tool for identifying potentially favorable mutations. This way, the computational effort for the identification of potentially stabilizing mutations with NEQ free energy calculations may be reduced.

Identification of stabilizing mutations using ddg monomer and NEQ free energy calculations

In the first two parts of this study, a model was built that could accurately predict the change in thermostability of DuraPETase upon single amino acid mutation. In the third part, it was also shown that *ddg monomer* calculations can be used to enrich promising mutations. We now decided to utilize these findings prospectively, to identify stabilizing mutations in addition to DuraPETase^{S42M}. To do so, $\Delta\Delta G_{folding}$ of another 60 variants was predicted. The entire workflow including the verification steps is summarized in Fig. 4. In accordance with the results presented above, the variants were randomly selected from the *low* group of *ddg monomer* predictions. Together with 40 already calculated mutations (Fig. 3), a total of 100 predictions were run. Out of these 100, the results of the calculations for four mutations could not be analyzed properly because the overlap in the work distribution for estimating ΔG was insufficient. In the end, this resulted in 96 successfully calculated $\Delta\Delta G_{folding}$ predictions (Fig. 5a). The top ranking 11 mutations all were

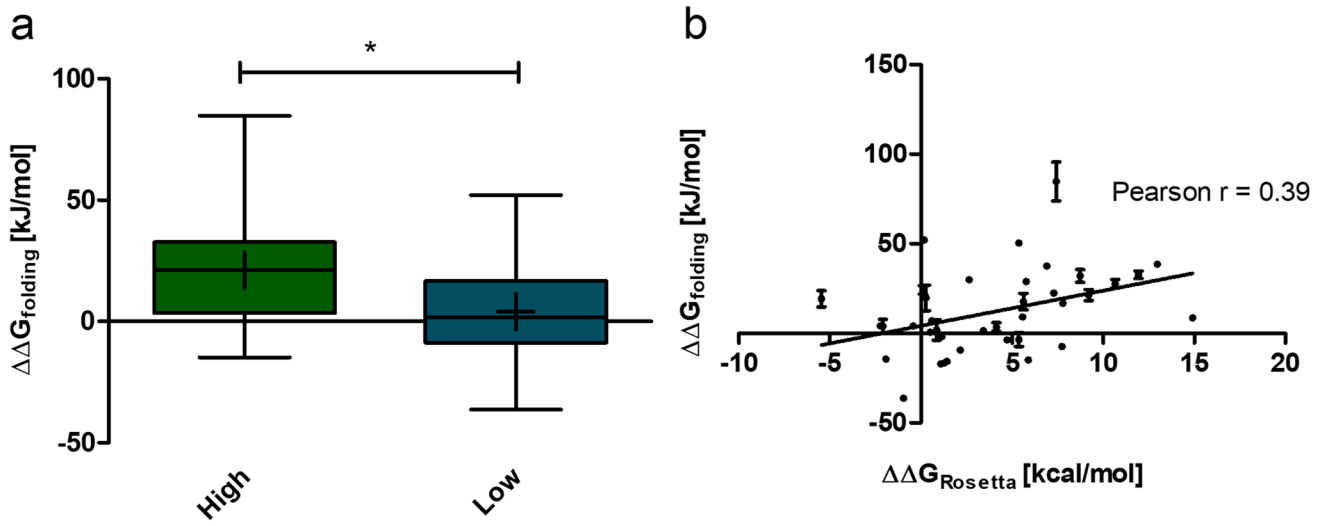

Fig. 3 **a** $\Delta\Delta G_{folding}$ predictions calculated with NEQ free energy calculations of 19 single amino acid mutations from the *high* and 20 single amino acid mutations from the *low ddg monomer* prediction subsets. The *high* subset was defined as predictions with a $\Delta\Delta G_{Rosetta} > 4$ kcal/mol. The *low* subset was defined as predictions with a $\Delta\Delta G_{Rosetta} < 4$ kcal/mol. The mean $\Delta\Delta G_{folding}$ was significantly lower for the *low* subset ($p = 0.013$), as indicated by an asterisk. **b** $\Delta\Delta G_{folding}$ predicted by NEQ free energy calculations plotted against the $\Delta\Delta G_{Rosetta}$ for single amino acid mutations. The error given for $\Delta\Delta G_{folding}$ is the standard deviation over four independent replicas. A significant Pearson correlation (Pearson $r = 0.39$, $p = 0.0145$, $N = 39$) of the $\Delta\Delta G_{Rosetta}$ and $\Delta\Delta G_{folding}$ values was observed

mutations to aromatic amino acids. To minimize potential bias, we decided to choose variants for experimental validation from among the top predictions as follows. A cutoff value of $\Delta\Delta G_{folding} = -6.5$ kJ/mol that corresponds to the calculated $\Delta\Delta G_{folding}$ of the already identified stabilizing DuraPETase^{S42M} variant was chosen. Nineteen variants were below this cutoff value. Ten variants were selected semi-randomly from these variants. However, the number of mutations to each single amino acid was limited to a maximum of three. The selected variants were expressed and purified and the T_m was measured by DSF (Fig. 5b). Two variants had significantly higher T_m than the original DuraPETase. Five variants had the same T_m as the original DuraPETase, while three variants had lower T_m. DuraPETase^{S223Y} was the most stable among all tested variants. The T_m was 0.93 °C higher than that of the original DuraPETase. DuraPETase^{A280W} had a T_m that was 2.30 °C lower than that of the original DuraPETase. It was the most unstable variant. The entire range of determined T_m from this screening was only 3.43 °C. This is distinctly smaller than in the first screening round that was based on *ddg monomer* predictions, which had a range of T_m of 21.66 °C. The number of mutations that were identified to be stabilizing with the second screening round was higher, two compared to one, even though the number of enzymes tested was smaller (10 instead of 13). There was however no significant correlation between the ΔT_m values and $\Delta\Delta G_{folding}$ for the variants from the second round screening ($r = -0.17$, $p = 0.63$, $N = 10$) (Fig. 5c). ΔT_m values of all 23 experimentally tested mutations were plotted against the calculated $\Delta\Delta G_{folding}$ (Fig. 5d). This resulted in a Pearson correlation of $r = -0.82$, which is slightly worse than the correlation determined for the first dataset alone. This shows that the prediction accuracy over the entire range of mutations is very good. When only focusing on stabilizing mutations, the prediction accuracy drops however. The lower accuracy of the predictions for stabilizing mutations also explains the slightly lower correlation of the entire dataset, when compared to the mutations from the first screening round alone. These results indicate that NEQ calculations predict $\Delta\Delta G_{folding}$ accurately as long as the mutation is not strongly stabilizing. With mutations predicted to be stabilizing, the effect seems to be overestimated. Stabilizing or neutral mutations are nevertheless enriched by the NEQ free energy calculations.

PET hydrolysis by DuraPETase variants

In addition to the already determined T_m for the ten DuraPETase variants from the second round of screening, their respective activities on amorphous PET were analyzed as well (Fig. 6). Since the variant DuraPETase^{S42M} from the first round was found to be stabilizing, it was also included. The activity was tested at 50 °C and 52 °C to see how the enzymes performed at the optimum temperature of the original DuraPETase (50 °C) and slightly above this temperature. Overall, the changes in activity at 50 °C and 52 °C reflect the observed changes in thermostability. DuraPETase^{S223Y}—which showed the strongest increase in

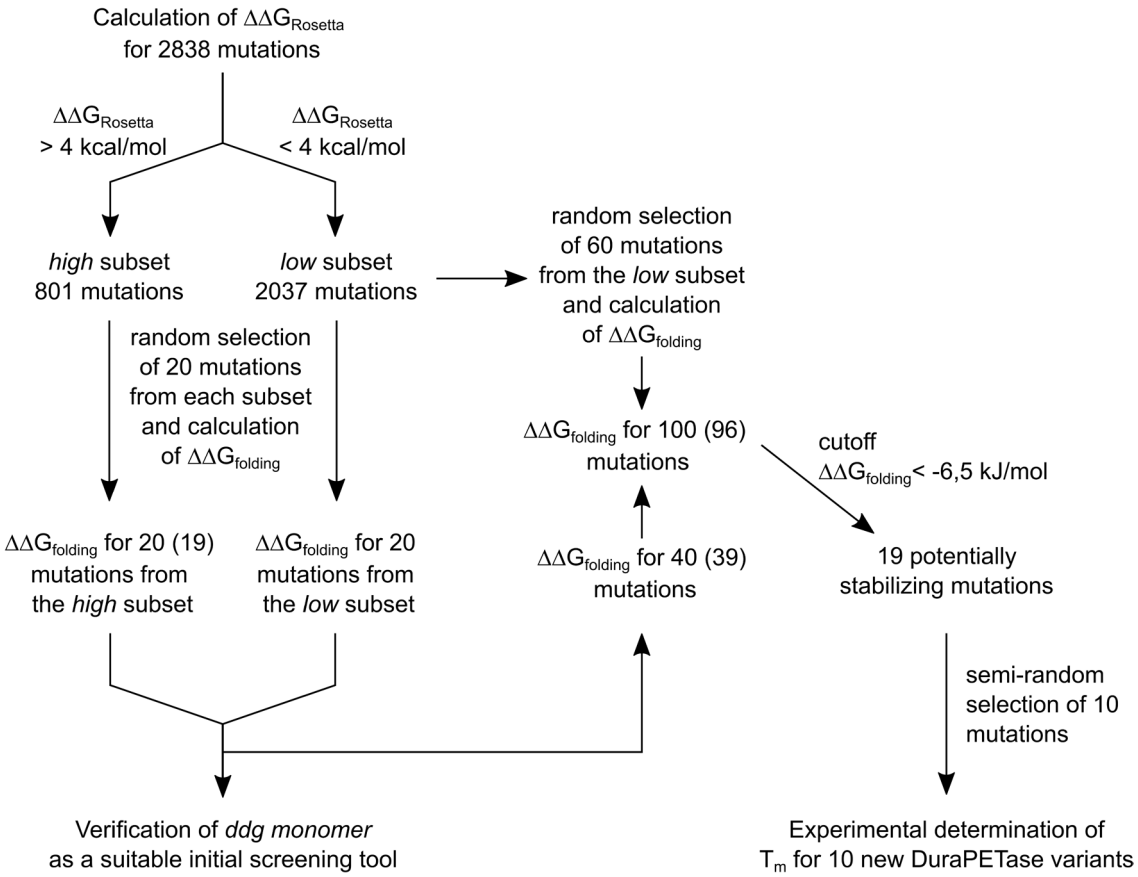

Fig. 4 Flow diagram of the complete workflow used in this study for the identification of more thermostable DuraPETase variants. Numbers shown in brackets show the actual number of successful run predictions, if it deviated from the initially intended number due to incomplete convergence in some of the predictions

T_m—showed practically identical PET degradation rates at 50 °C compared to the original DuraPETase but was approx. ten percent more active at 52 °C. Similarly, a better performance at 52 °C was also recorded for one of the other two more thermostable variants, DuraPETase^{S42M}. For the third stable variant, DuraPETase^{S61M}, the same tendency was observed at 52 °C, the results were however not statistically significant. The variants DuraPETase^{G75I}, DuraPETase^{A280W}, and DuraPETase^{A280Q} all showed a reduced thermostability. In line with this, there was a pronounced decrease of PET degradation rates at 50 °C for these variants. The overall changes in thermostability of the new variants were relatively small compared to the already very high T_m of original DuraPETase. In line with this, only relatively small changes could be measured when analyzing the PET degradation activity at a temperature slightly above the original optimum temperature.

Discussion

In this study, a workflow for the improvement of enzyme thermostability based around the Rosetta *ddg monomer* tool and NEQ alchemical free energy calculations was developed. DuraPETase, the enzyme optimized in this study, is a highly evolved thermostable enzyme (Cui et al. 2021) and therefore an interesting test case for the performance and limitations of the NEQ alchemical free energy calculation approach. Alchemical free energy calculations have been established as a powerful tool for predicting the change in protein stability upon amino acid mutation (Gapsys et al. 2016; Steinbrecher et al. 2017b). They therefore provide the opportunity to reduce the number of enzyme variants that need to be tested experimentally. The high computational demand of free energy calculations has however limited their use in prospective studies.

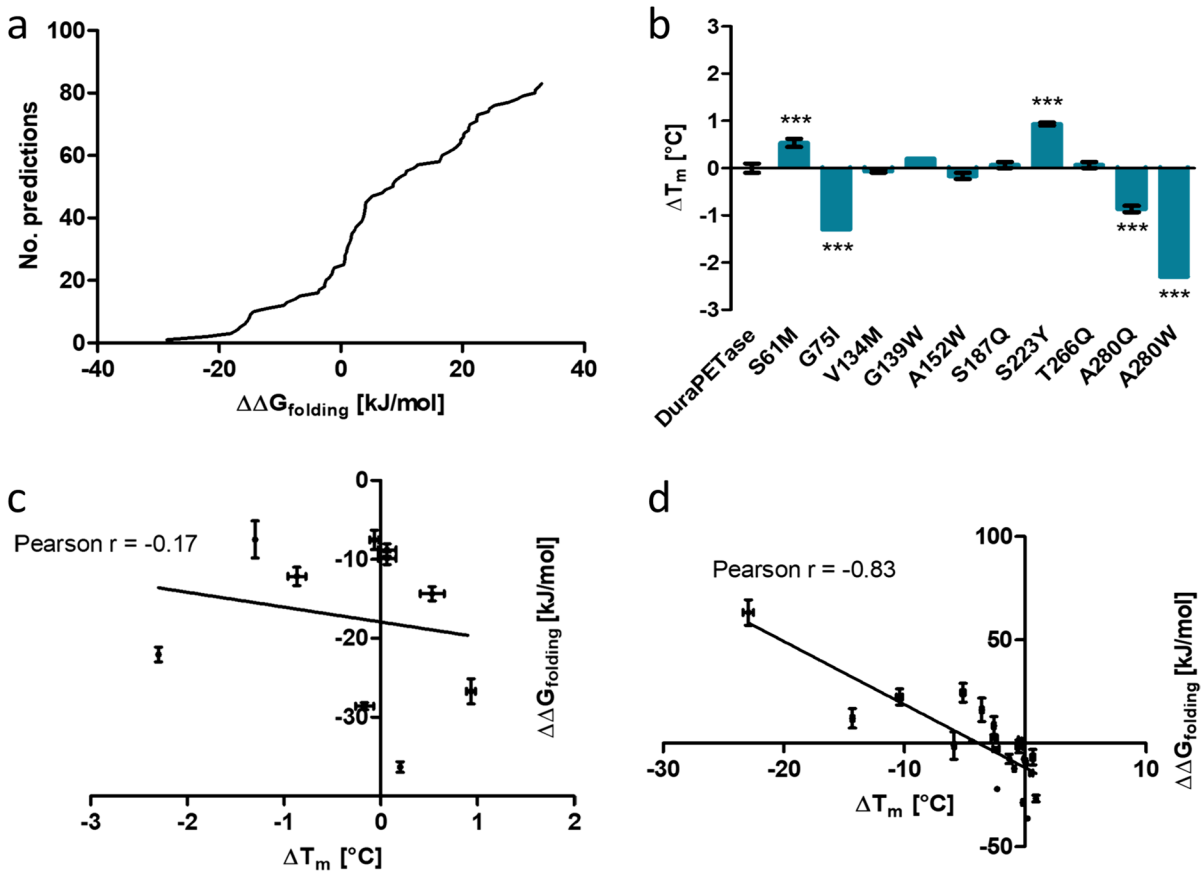

Fig. 5 **a** Cumulative distribution of $\Delta\Delta G_{folding}$ calculated with NEQ free energy calculations for single amino acid mutations of DuraPETase. Eighty mutations were selected from the *low* subset of predictions from the *ddg monomer* results, while 20 were chosen from the *high* subset. For four mutations, insufficient overlap in the work distribution for estimating ΔG was observed. They were excluded from further analysis. In total, the results of 96 predictions are shown. **b** ΔT_m of different purified DuraPETase variants. ΔT_m were calculated by subtracting the T_m value of the original DuraPETase from the T_m value of each respective variant. T_m values were determined by DSF. The variants were selected among mutations predicted to have $\Delta\Delta G_{folding}$ less than − 6.5 kJ/mol calculated with NEQ free energy calculations. **c** Experimentally determined ΔT_m values plotted against $\Delta\Delta G_{folding}$ values calculated by NEQ free energy calculations of ten DuraPETase variants from the second round of screening. No significant correlation of the ΔT_m values and $\Delta\Delta G_{folding}$ values was observed (Pearson r = -0.17, p = 0.63, N = 10). **d** Experimentally determined ΔT_m values plotted against $\Delta\Delta G_{folding}$ values calculated by NEQ free energy calculations of 23 DuraPETase variants from both rounds of screening. A significant negative correlation of ΔT_m values and $\Delta\Delta G_{folding}$ values was observed (Pearson r = -0.83, $p < 0.0001$, N = 23). The uncertainty given for ΔT_m is the standard deviation of three independent measurements. Statistical significance was analyzed by one-way ANOVA with Dunnett's multiple comparison test. Triple asterisk (***) corresponds to $p < 0.001$. The uncertainty of $\Delta\Delta G_{folding}$ for each mutation is the standard deviation of four independent replicas

This study demonstrates how to integrate free energy calculations into a protein engineering project to supplement well-established semi-empirical in silico methods (Bell et al. 2022; Cui et al. 2021). The use of the *ddg monomer* tool in the first round of screening resulted in the identification of a single DuraPETase variant with higher thermostability among 13 tested variants. Compared with previous results also using semi-empirical methods, this is on the lower end of successful predictions (Buß et al. 2018; Wijma et al. 2018). The outcome was however potentially better than the expected 2% success rate in a directed evolutionary approach (Bromberg and Rost 2009). Due to the rather small sample size, this is just a rough approximation and cannot be judged reliably. The NEQ alchemical free energy calculations performed next, resulted in a very good correlation between the experimentally measured T_m and the predicted $\Delta\Delta G_{folding}$. Pearson's correlation coefficient was − 0.85. Linear regression gave an $R^2 = 0.73$. Notably, T_m is not a direct measure for $\Delta G_{unfolding}$ at standard conditions (Peccati et al. 2023). Nevertheless, the correlation between T_m and $\Delta G_{unfolding}$ generally is extremely high (Gapsys et al. 2016; Wijma et al. 2014). Pearson's correlation coefficient for the ΔT_m and changes in folding free energy falls within the same range as the previously reported excellent correlation of $r = 0.86$ determined with the same approach (Gapsys et al. 2016). Studies employing equilibrium free

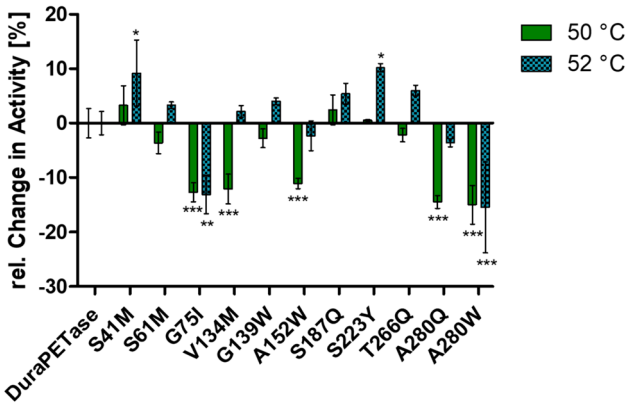

Fig. 6 Relative activity alterations of DuraPETase variants at 50 °C and 52 °C in comparison to the original DuraPETase. The purified enzymes were used at 100 nmol/l and incubated for 3 days at 50 °C or 52 °C in 300 µl of 50 mmol/l bicine NaOH buffer pH 9 with a 6 mm diameter cutout of amorphous PET. The PET degradation activity was quantified by determining the concentration of the reaction products by HPLC. The changes in activity are given as relative values and are normalized to the PET degradation rates for the original DuraPETase at 50 °C and 52 °C, respectively. All experiments were performed as triplicates. Statistical significance was analyzed by one-way ANOVA with Dunnett's multiple comparison test against the DuraPETase sample at the corresponding temperature. Triple asterisk (***) corresponds to $p < 0.001$, double asterisk (**) corresponds to $p < 0.01$, and single asterisk (*) corresponds to $p < 0.05$

energy perturbations (FEP) reported on slightly worse R^2 of 0.4 and 0.65 compared to the R^2 of 0.73 reported in this study for the correlation between experimentally and predicted $\Delta\Delta G_{\text{unfolding}}$ (Jespers et al. 2019; Scarabelli et al. 2022; Steinbrecher et al. 2017b). One reason for the high correlation between T_m and $\Delta\Delta G_{\text{unfolding}}$ in our dataset might be the fact that we excluded charge changing mutations from our predictions. Charge change mutations have been shown to converge slower and are predicted less accurately by both NEQ and EQ alchemical free energy calculations (Clark et al. 2019; Patel et al. 2021). Purposefully omitting them might therefore increase the prediction accuracy.

With the intent to combine the *ddg monomer* tool and NEQ alchemical free energy calculations in the second screening round, it was first shown that the *ddg monomer* tool can enrich stabilizing mutations. Selection of mutations from a subset of possible mutations with lower $\Delta\Delta G_{\text{Rosetta}}$ led to an on average lower $\Delta\Delta G_{\text{folding}}$ predicted by NEQ alchemical free energy calculations. This shows that mutations with lower scores from the *ddg monomer* tool should be prioritized for free energy calculations. This two-step approach has the potential to save significant amounts of computational time while simultaneously enabling the screening of large portions of the sequence space. Out of a total of 96 NEQ alchemical free energy calculations, 19 were below a cutoff of − 6.5 kJ/mol. Out of these 19, 11 were mutations to aromatic amino acids. These mutations are generally considered to be stabilizing (Serrano et al. 1991). Aromatic amino acids thermodynamically favor the folded state of a protein, as this minimizes the solvent exposed hydrophobic surface area and enables hydrophobic interactions between the amino acids. It is however also possible that the stabilizing effect of aromatic amino acids might be overestimated by the NEQ alchemical free energy calculations, due to insufficient sampling or force field inaccuracies. This is also why we limited the experimental validation of variants to a maximum of three variants for a mutation into any single amino acid.

Ten of the variants predicted to be stabilizing in the second screening round were tested experimentally. No significant correlation between experimental and predicted values was observed for these ten variants. The prediction accuracy over the entire dataset of 23 mutations was however still good, with a Pearson's correlations coefficient of $r = -0.83$. This indicates a better performance of the NEQ alchemical free energy calculations for destabilizing and neutral mutations and a worse prediction accuracy for stabilizing ones. In contrast to these findings, previous studies have shown that the correlation between experimental and predicted $\Delta\Delta G_{\text{folding}}$ is roughly the same for stabilizing and destabilizing mutations (Gapsys et al. 2016; Steinbrecher et al. 2017b). Naturally occurring proteins, as used in the datasets of theses previous studies, are most often mesophilic and only marginally stable (Goldenzweig and Fleishman 2018; Taverna and Goldstein 2002). DuraPETase, with its T_m of 78 °C, is however already highly thermostable. From this, the question arises, if the performance of NEQ free alchemical free energy calculations is worse for single amino acid mutations that further increase the stability of already highly stable proteins. Theoretically, this should not be the case, as NEQ alchemical free energy calculations present a physically rigorous way of calculating changes in protein folding free energy. Insufficient sampling during the MD simulation can however influence the accuracy of the predictions. Highly stable proteins are often more rigid, and transitions between relevant conformations might take more time, because they are separated from each other by higher energy barriers. Thorough sampling of all relevant conformations for highly stable proteins might therefore take more time than for less stable ones. This directly impacts the accuracy of the free energy prediction, as it is dependent on a correct frequency distribution of all relevant conformations. Performing multiple independent replicas, as done in this study, should provide a first indication if insufficient sampling poses a problem in the system under investigation. If, however, the number of replicas is too small and relevant conformations are only marginally populated, this approach might nevertheless provide a false error estimate. A convenient way to detect such limitations during MD sampling could be the usage of closed thermodynamic cycles with

relative free energy differences at their edges. If the sum of all relative free energy changes deviates from zero, insufficient sampling for one or multiple of the mutations could be an issue (Gapsys et al. 2015a; Hardebeck et al. 2023). Both approaches mentioned above, the use of closed thermodynamic cycle and increasing the number of independent replicas, come however with a substantial increase in computational effort and need to be considered carefully. Aside from potential sampling issues, force field parametrization also influences the performance of NEQ alchemical free energy calculations (Gapsys et al. 2016). The force fields used in molecular simulations are typically parameterized based on experimental data and may not fully capture the nuances of highly stable proteins (Lindorff-Larsen et al. 2010). To the best of our knowledge, a comprehensive investigation on the performance of force fields on highly stable proteins has not been undertaken thus far. This could be an interesting topic for future research in the context of the application of free energy calculations.

Overall, we managed to identify three mutations that increased the thermostability of DuraPETase. The increase in thermostability was however limited, especially when compared with other optimizations of IsPETase (Bell et al. 2022; Cui et al. 2021; Lu et al. 2022). It is also a rather limited number of successfully identified mutations when compared to another protein engineering project. Song et al. used the well-established FoldX tool in conjunction with a free energy perturbation approach for the engineering of a more thermostable blue light photo receptor YtvA LOV domain from *Bacillus subtilis*. They identified nine stabilizing mutations and had a good correlation of $r=0.63$ between experimentally determined and predicted $\Delta\Delta G$ values (Song et al. 2013). When one however considers the free energy surface as a function of protein sequence space, it is conceivable that several local minima exist in addition to the global minimum. If the sequence of DuraPETase represents a point close to such a local minimum on the energy hypersurface, only small increases in thermostability can be achieved by single amino acid mutations. This is consistent with reports in the literature where larger enhancement in the thermostability of DuraPETase was only achieved with the introduction of a disulfide bond or a salt bridge (Brott et al. 2022; Lu et al. 2022). Both are mutations that could not have been identified with our screening approach.

The three mutations identified with the screening approach with a higher T_m than original DuraPETase were DuraPETase^{S42M}, DuraPETase^{S61M}, and DuraPETase^{S223Y}. None of these mutations are located near the active center. Interestingly, in the thermostable PETase variant HotPETase, the serine in position 61 was also mutated, however in this case to a valine (Bell et al. 2022). Both mutations introduce more lipophilic amino acids. The serine is located near the surface of the enzyme in a relatively hydrophilic region. Introduction of a hydrophobic residue in this region likely leads to a more compact packing of the region to reduce the surface exposed hydrophobic area. This could pose a possible explanation for the increased thermostability of the enzyme. The same explanation can be given for DuraPETase^{S61M} and DuraPETase^{S223Y}. Serine 61 and serine 223 are also located near the surface of the enzyme, and mutation to a methionine or tyrosine also drastically increases the lipophilicity at these positions. Analysis of PET hydrolysis by the DuraPETase variants showed that variants with an improved thermostability also were more active than the original DuraPETase at an elevated reaction temperature of 52 °C. The most stable variant DuraPETase^{S223Y} showed the highest amount of PET degradation at 52 °C with a 10% increase compared to the original DuraPETase. If this can be attributed to an increased activity or a longer half-life of the enzyme at 52 °C remains unclear. Unfortunately, this slight increase in both the T_m and the improved degradation rate at 52 °C of the variant is likely not relevant for the potential industrial application of DuraPETase.

In conclusion, we demonstrated the applicability of NEQ alchemical free energy calculations for enzyme engineering projects. Challenges encountered with the extremely stable DuraPETase in this study, however, also highlight limitations of the approach and provide directions for the further optimization and validation of free energy calculations. We also validated an efficient way to integrate NEQ alchemical free energy calculations with semi-empirical methods to reduce overall computational cost. Overall, this study shows that free energy calculations can be a valuable tool for the design of thermostable proteins that can be readily employed in these kinds of projects.

Supplementary Information The online version contains supplementary material available at https://doi.org/10.1007/s00253-024-13144-z.

Acknowledgements We acknowledge the support of the HPC facility of the University of Münster for providing computational resources.

Author contribution SS and DG contributed equally to this work. SS and DG performed experiments and data analysis. FL performed data analysis. SN, DG, and JJ conceived and designed research. SS and DG wrote the initial manuscript. FL and JJ reviewed and edited the manuscript. JJ supervised the research and acquired funding. All authors have read and approved the final version of the manuscript.

Funding Open Access funding enabled and organized by Projekt DEAL.

Data availability Data is available from the corresponding author upon reasonable request.

Declarations

Ethics approval This article does not contain any studies with human participants or animals performed by any of the authors.

Competing interests The authors declare no competing interest.

References

Abraham MJ, Murtola T, Schulz R, Páll S, Smith JC, Hess B, Lindahl E (2015) GROMACS: high performance molecular simulations through multi-level parallelism from laptops to supercomputers. SoftwareX 1–2:19–25. https://doi.org/10.1016/j.softx.2015.06.001

Aldeghi M, de Groot BL, Gapsys V (2019) Accurate calculation of free energy changes upon amino acid mutation. Methods Mol Biol 1851:19–47. https://doi.org/10.1007/978-1-4939-8736-8_2

Bell EL, Smithson R, Kilbride S, Foster J, Hardy FJ, Ramachandran S, Tedstone AA, Haigh SJ, Garforth AA, Day PJR, Levy C, Shaver MP, Green AP (2022) Directed evolution of an efficient and thermostable PET depolymerase. Nat Catal 5(8):673–681. https://doi.org/10.1038/s41929-022-00821-3

Bennett CH (1976) Efficient estimation of free energy differences from Monte Carlo data. J Comput Phys 22(2):245–268. https://doi.org/10.1016/0021-9991(76)90078-4

Bhati AP, Coveney PV (2022) Large scale study of ligand–protein relative binding free energy calculations: actionable predictions from statistically robust protocols. J Chem Theory Comput 18(4):2687–2702. https://doi.org/10.1021/acs.jctc.1c01288

Bommarius AS, Blum JK, Abrahamson MJ (2011) Status of protein engineering for biocatalysts: how to design an industrially useful biocatalyst. Curr Opin Chem Biol 15(2):194–200. https://doi.org/10.1016/j.cbpa.2010.11.011

Bromberg Y, Rost B (2009) Correlating protein function and stability through the analysis of single amino acid substitutions. BMC Bioinformatics 10(8):S8. https://doi.org/10.1186/1471-2105-10-S8-S8

Brott S, Pfaff L, Schuricht J, Schwarz JN, Bottcher D, Badenhorst CPS, Wei R, Bornscheuer UT (2022) Engineering and evaluation of thermostable IsPETase variants for PET degradation. Eng Life Sci 22(3–4):192–203. https://doi.org/10.1002/elsc.202100105

Buß O, Rudat J, Ochsenreither K (2018) FoldX as protein engineering tool: better than random based approaches? Comput Struct Biotechnol J 16:25–33. https://doi.org/10.1016/j.csbj.2018.01.002

Bussi G, Donadio D, Parrinello M (2007) Canonical sampling through velocity rescaling. J Chem Phys 126(1):014101. https://doi.org/10.1063/1.2408420

Childers MC, Daggett V (2017) Insights from molecular dynamics simulations for computational protein design. Mol Syst Des Eng 2(1):9–33. https://doi.org/10.1039/C6ME00083E

Clark AJ, Negron C, Hauser K, Sun M, Wang L, Abel R, Friesner RA (2019) Relative binding affinity prediction of charge-changing sequence mutations with FEP in protein–protein interfaces. J Mol Biol 431(7):1481–1493. https://doi.org/10.1016/j.jmb.2019.02.003

Crooks GE (1999) Entropy production fluctuation theorem and the nonequilibrium work relation for free energy differences. Phys Rev E 60(3):2721–2726. https://doi.org/10.1103/PhysRevE.60.2721

Cui Y, Chen Y, Liu X, Dong S, Ye T, Qiao Y, Mitra R, Han J, Li C, Han X, Liu W, Chen Q, Wei W, Wang X, Du W, Tang S, Xiang H, Liu H, Liang Y, Houk KN, Wu B (2021) Computational redesign of a PETase for plastic biodegradation under ambient condition by the GRAPE strategy. ACS Catal 11(3):1340–1350. https://doi.org/10.1021/acscatal.0c05126

Dehouck Y, Grosfils A, Folch B, Gilis D, Bogaerts P, Rooman M (2009) Fast and accurate predictions of protein stability changes upon mutations using statistical potentials and neural networks: PoPMuSiC-2.0. Bioinformatics 25(19):2537–2543. https://doi.org/10.1093/bioinformatics/btp445

Essmann U, Perera L, Berkowitz ML, Darden T, Lee H, Pedersen LG (1995) A smooth particle mesh Ewald method. J Chem Phys 103(19):8577–8593. https://doi.org/10.1063/1.470117

Floor RJ, Wijma HJ, Colpa DI, Ramos-Silva A, Jekel PA, Szymański W, Feringa BL, Marrink SJ, Janssen DB (2014) Computational library design for increasing haloalkane dehalogenase stability. ChemBioChem 15(11):1660–1672. https://doi.org/10.1002/cbic.201402128

Ford MC, Babaoglu K (2017) Examining the feasibility of using free energy perturbation (FEP+) in predicting protein stability. J Chem Inf Model 57(6):1276–1285. https://doi.org/10.1021/acs.jcim.7b00002

Gapsys V, Michielssens S, Peters JH, de Groot BL, Leonov H (2015a) Calculation of binding free energies. In: Kukol A (ed) Molecular modeling of proteins. Springer, New York, New York, NY, pp 173–209

Gapsys V, Michielssens S, Seeliger D, de Groot BL (2015b) pmx: automated protein structure and topology generation for alchemical perturbations. J Comput Chem 36(5):348–354. https://doi.org/10.1002/jcc.23804

Gapsys V, Michielssens S, Seeliger D, de Groot BL (2016) Accurate and rigorous prediction of the changes in protein free energies in a large-scale mutation scan. Angew Chem Int Ed Engl 55(26):7364–7368. https://doi.org/10.1002/anie.201510054

Goldenzweig A, Fleishman SJ (2018) Principles of protein stability and their application in computational design. Annu Rev Biochem 87(1):105–129. https://doi.org/10.1146/annurev-biochem-062917-012102

Guerois R, Nielsen JE, Serrano L (2002) Predicting changes in the stability of proteins and protein complexes: a study of more than 1000 mutations. J Mol Biol 320(2):369–387. https://doi.org/10.1016/S0022-2836(02)00442-4

Hardebeck S, Schreiber S, Adick A, Langer K, Jose J (2023) A FRET-based assay for the identification of PCNA inhibitors. Int J Mol Sci 24(14):11858

Hess B, Bekker H, Berendsen HJC, Fraaije JGEM (1997) LINCS: a linear constraint solver for molecular simulations. J Comput Chem 18(12):1463–1472. https://doi.org/10.1002/(SICI)1096-987X(199709)18:12%3c1463::AID-JCC4%3e3.0.CO;2-H

Jarzynski C (1997a) Equilibrium free-energy differences from nonequilibrium measurements: a master-equation approach. Phys Rev E 56(5):5018–5035. https://doi.org/10.1103/PhysRevE.56.5018

Jarzynski C (1997b) Nonequilibrium equality for free energy differences. Phys Rev Lett 78(14):2690–2693. https://doi.org/10.1103/PhysRevLett.78.2690

Jespers W, Isaksen GV, Andberg TAH, Vasile S, van Veen A, Åqvist J, Brandsdal BO, Gutiérrez-de-Terán H (2019) QresFEP: an automated protocol for free energy calculations of protein mutations in Q. J Chem Theory Comput 15(10):5461–5473. https://doi.org/10.1021/acs.jctc.9b00538

Jog JP (1995) Crystallization of polyethyleneterephthalate. JMS Rev Macromol Chem Phys 35(3):531–553. https://doi.org/10.1080/15321799508014598

Kellogg EH, Leaver-Fay A, Baker D (2011) Role of conformational sampling in computing mutation-induced changes in protein structure and stability. Proteins 79(3):830–838. https://doi.org/10.1002/prot.22921

Labrou NE (2010) Random mutagenesis methods for in vitro directed enzyme evolution. Curr Protein Pept Sci 11(1):91–100. https://doi.org/10.2174/138920310790274617

Lavinder JJ, Hari SB, Sullivan BJ, Magliery TJ (2009) High-throughput thermal scanning: a general, rapid dye-binding thermal shift screen for protein engineering. J Am Chem Soc 131(11):3794–3795. https://doi.org/10.1021/ja8049063

Lindorff-Larsen K, Piana S, Palmo K, Maragakis P, Klepeis JL, Dror RO, Shaw DE (2010) Improved side-chain torsion potentials for the Amber ff99SB protein force field. Proteins 78(8):1950–1958. https://doi.org/10.1002/prot.22711

Liu Y, Liu Z, Guo Z, Yan T, Jin C, Wu J (2022) Enhancement of the degradation capacity of IsPETase for PET plastic degradation by protein engineering. Sci Total Environ 834:154947. https://doi.org/10.1016/j.scitotenv.2022.154947

Lu H, Diaz DJ, Czarnecki NJ, Zhu C, Kim W, Shroff R, Acosta DJ, Alexander BR, Cole HO, Zhang Y, Lynd NA, Ellington AD, Alper HS (2022) Machine learning-aided engineering of hydrolases for PET depolymerization. Nature 604(7907):662–667. https://doi.org/10.1038/s41586-022-04599-z

Nezhad NG, Rahman R, Normi YM, Oslan SN, Shariff FM, Leow TC (2022) Thermostability engineering of industrial enzymes through structure modification. Appl Microbiol Biotechnol 106(13–16):4845–4866. https://doi.org/10.1007/s00253-022-12067-x

Parrinello M, Rahman A (1981) Polymorphic transitions in single crystals: a new molecular dynamics method. J Appl Phys 52(12):7182–7190. https://doi.org/10.1063/1.328693

Patel D, Patel JS, Ytreberg FM (2021) Implementing and assessing an alchemical method for calculating protein-protein binding free energy. J Chem Theory Comput 17(4):2457–2464. https://doi.org/10.1021/acs.jctc.0c01045

Peccati F, Alunno-Rufini S, Jiménez-Osés G (2023) Accurate prediction of enzyme thermostabilization with Rosetta using AlphaFold ensembles. J Chem Inf Model 63(3):898–909. https://doi.org/10.1021/acs.jcim.2c01083

Scarabelli G, Oloo EO, Maier JKX, Rodriguez-Granillo A (2022) Accurate prediction of protein thermodynamic stability changes upon residue mutation using free energy perturbation. J Mol Biol 434(2):167375. https://doi.org/10.1016/j.jmb.2021.167375

Seeliger D, de Groot BL (2010) Protein thermostability calculations using alchemical free energy simulations. Biophys J 98(10):2309–2316. https://doi.org/10.1016/j.bpj.2010.01.051

Serrano L, Bycroft M, Fersht AR (1991) Aromatic-aromatic interactions and protein stability: investigation by double-mutant cycles. J Mol Biol 218(2):465–475. https://doi.org/10.1016/0022-2836(91)90725-L

Shi L, Liu P, Tan Z, Zhao W, Gao J, Gu Q, Ma H, Liu H, Zhu L (2023) Complete depolymerization of pet wastes by an evolved PET hydrolase from directed evolution. Angew Chem Int Ed 62(14):e202218390. https://doi.org/10.1002/anie.202218390

Shirts MR, Chodera JD (2008) Statistically optimal analysis of samples from multiple equilibrium states. J Chem Phys 129(12):124105. https://doi.org/10.1063/1.2978177

Shirts MR, Bair E, Hooker G, Pande VS (2003) Equilibrium free energies from nonequilibrium measurements using maximum-likelihood methods. Phys Rev Lett 91(14):140601. https://doi.org/10.1103/PhysRevLett.91.140601

Song X, Wang Y, Shu Z, Hong J, Li T, Yao L (2013) Engineering a more thermostable blue light photo receptor *Bacillus subtilis* YtvA LOV domain by a computer aided rational design method. PLoS Comp Biol 9(7):e1003129. https://doi.org/10.1371/journal.pcbi.1003129

Steinbrecher T, Abel R, Clark A, Friesner R (2017a) Free energy perturbation calculations of the thermodynamics of protein side-chain mutations. J Mol Biol 429(7):923–929. https://doi.org/10.1016/j.jmb.2017.03.002

Steinbrecher T, Zhu C, Wang L, Abel R, Negron C, Pearlman D, Feyfant E, Duan J, Sherman W (2017b) Predicting the effect of amino acid single-point mutations on protein stability—large-scale validation of MD-based relative free energy calculations. J Mol Biol 429(7):948–963. https://doi.org/10.1016/j.jmb.2016.12.007

Taverna DM, Goldstein RA (2002) Why are proteins marginally stable? Proteins 46(1):105–109. https://doi.org/10.1002/prot.10016

Wang X-C, You S-P, Zhang J-X, Dai Y-M, Zhang C-Y, Qi W, Dou T-Y, Su R-X, He Z-M (2018) Rational design of a thermophilic β-mannanase from *Bacillus subtilis* TJ-102 to improve its thermostability. Enzyme Microb Technol 118:50–56. https://doi.org/10.1016/j.enzmictec.2018.07.005

Wei R, Zimmermann W (2017) Biocatalysis as a green route for recycling the recalcitrant plastic polyethylene terephthalate. Microb Biotechnol 10(6):1302–1307. https://doi.org/10.1111/1751-7915.12714

Wijma HJ, Floor RJ, Jekel PA, Baker D, Marrink SJ, Janssen DB (2014) Computationally designed libraries for rapid enzyme stabilization. Protein Eng Des Sel 27(2):49–58. https://doi.org/10.1093/protein/gzt061

Wijma HJ, Fürst MJLJ, Janssen DB (2018) A computational library design protocol for rapid improvement of protein stability: FRESCO. In: Bornscheuer UT, Höhne M (eds) Protein engineering: methods and protocols. Springer, New York, New York, NY, pp 69–85

Yoshida S, Hiraga K, Takehana T, Taniguchi I, Yamaji H, Maeda Y, Toyohara K, Miyamoto K, Kimura Y, Oda K (2016) A bacterium that degrades and assimilates poly(ethylene terephthalate). Science 351(6278):1196–1199. https://doi.org/10.1126/science.aad6359

Zurier HS, Goddard JM (2023) A high-throughput expression and screening platform for applications-driven PETase engineering. Biotechnol Bioeng 120(4):1000–1014. https://doi.org/10.1002/bit.28319

Zwanzig RW (1954) High-temperature equation of state by a perturbation method. I Nonpolar Gases J Chem Phys 22(8):1420–1426. https://doi.org/10.1063/1.1740409